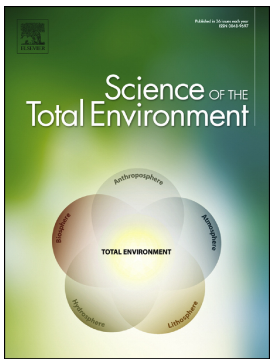

Impact of land use changes on flash flood prediction using a sub-daily SWAT model in five Mediterranean ungauged watersheds (SE Spain)

Antonio Jodar-Abellan, Javier Valdes-Abellan, Concepción Pla, Francisco Gomariz-Castillo

PII: S0048-9697(18)34871-X
DOI: https://doi.org/10.1016/j.scitotenv.2018.12.034
Reference: STOTEN 29868

To appear in: *Science of the Total Environment*

Received date: 19 October 2018
Revised date: 3 December 2018
Accepted date: 4 December 2018

Please cite this article as: Antonio Jodar-Abellan, Javier Valdes-Abellan, Concepción Pla, Francisco Gomariz-Castillo , Impact of land use changes on flash flood prediction using a sub-daily SWAT model in five Mediterranean ungauged watersheds (SE Spain). Stoten (2018), https://doi.org/10.1016/j.scitotenv.2018.12.034

Impact of land use changes on flash flood prediction using a Sub-daily SWAT model in five Mediterranean ungauged watersheds (SE Spain).

Antonio Jodar-Abellan[1], Javier Valdes-Abellan[1,2], Concepción Pla[1,2], & Francisco Gomariz-Castillo[3].

[1]*University institute of Water and Environmental Sciences. University of Alicante (Spain).*

antonio.jodar@ua.es

[2]*Department of Civil Engineering. University of Alicante (Spain).*

[3]*Euro-Mediterranean Water Institute. University of Murcia (Spain).*

HIGHLIGHTS

• High urban development in the coastline of SE Spain increases curve number rates (80-90).

• In Mediterranean convective systems, some precipitation episodes surpass 200-300 mm in three or four hours.

• Flash floods simulations, through the SWAT code, reported discharge rates which exceed 900 m^3/s.

• Peak flow rates have doubled or tripled as a consequence of changes in the land use during last decades.

• Improving hydraulic barriers and socio-environmental risk perception against flash floods effects is mandatory.

GRAPHICAL ABSTRACT

ABSTRACT

Flash floods cause severe natural disasters over the world generating property and infrastructures damages, poverty and loss of human life, among others. Mediterranean coastal watersheds are specially sensible to flash floods effects due to their typical drainage basin features (steep slopes, short concentration times, complex orography, etc.) and the high rainfall intensity typical of convective systems. In the present study, the temporal evolution of the hydrological answer in five Mediterranean (SE Spain) ravine basins with sizes from 10.2 km^2 to 200.9 km^2 were analysed. A sub-daily SWAT model was used at watershed scale to capture the complex hydrological dynamics. Five land use scenarios corresponding to no-urbanization

(baseline), 1990, 2000, 2006 and 2012 were evaluated using GIS-based tools. Additionally, statistical significant differences among the studied scenarios were checked employing the Kruskal-Wallis and post-hoc tests based on Mann-Whitney test with BH correction.

Our results show that flash flood risks have increased in the studied catchments due to changes in land uses, particularly affected by a large urban growth. Observed changes in soil uses have been important since the sixties of the last century, because of a high demographic and touristic pressure and specially the urban area has enhanced considerably during the last 22 years. Currently, some of these catchments present around 70% of their surface occupied by urban land uses with high population density producing curve number surpasses 85 and 90 levels. The hydrological response of the studied basins changed to higher flow rate peaks and shorter concentration times. Some discharges increased significantly from the baseline land use scenario (≈ 50 m^3/s, 190 m^3/s, 380 m^3/s) to the most urbanised scenario (≈ 235 m^3/s, 385 m^3/s, 940 m^3/s), respectively. These findings provide to urban planning policy makers very useful information in the face of flash flood effects, which have cost even human lifes in the studied ravine basins during last years.

Keywords: Land use changes; urban development; flash floods; SWAT; sub-daily simulation; Mediterranean ravine basins.

1. Introduction

Flash floods are one of the main risks that humans have faced throughout history. Particularly in highly inhabited regions, flash floods produce some of the most sever natural hazards as high peak runoff rates, landslides, transport of sediments and contaminants, causing destruction to property, infrastructures, damage in agricultural crops, livestock death, poverty, and even loss of human life (Boithias et al., 2017; Hooke, 2016; Mahmood et al., 2017). Flash floods increase population vulnerability and, therefore, socio-environmental risk (Nogueira de Andrade and Szlafsztein, 2018; Olcina-Cantos et al., 2010). Main factors affecting flash flood occurrence are rainfall characteristics (duration, total amount, intensity, time-space distribution, etc.) and drainage basin features (surface, length, slopes, time of concentration, orography, land use and soils types and/or vegetation). Detailed information about the flash floods concepts,

their differences with common floods, and associated factors can be found in Nogueira de Andrade and Szlafsztein (2018), Ballesteros et al. (2018), Camarasa-Belmonte et al. (2011), Conesa-García et al. (2017), Rozalis et al. (2010), Zhong et al. (2018), etc.

This situation is particularly common in certain arid and semi-arid Mediterranean areas such as Southeast of Spain, where one of its climate features is the presence of convective storms with very quick development, short duration and very high intensity. These rain episodes constitute a potential threat (Boithias et al., 2017; Martínez-Ibarra, 2012; Papagiannaki et al., 2015; Valdes-Abellan et al., 2017). At the same time, land use in the region has changed significantly, characterised by a great urbanization and occupation, specially supported by the touristic activity. This large urbanization and temporal population growth is mainly concentrated in the coastline of the Mediterranean basins and spreads flash flood risk due to the raise of impervious areas, the reduction in flood propagation times and infiltration rates and, consequently, increasing peak runoff rates (Camarasa-Belmonte et al., 2011; Jeong et al., 2010; Pérez-González et al., 2017). In addition, rainfall intensities and land use changes are related because of, for example, urban areas modify regional climate through several alterations into the albedo, greenhouse-effect emissions, etc. varying the water balances and surface energy. Moreover, at the end of the summer the warm water surface temperature of the Mediterranean Sea raises the convective energy of the superimposed air masses and the complex topography from these coastal areas increases the moist convection (Amengual et al., 2015; Ballesteros et al., 2018), leading to very high intensity rainfall events. Consequences of this situation have been widely identified in many studies along most affected provinces in the Southeast of Spain as Almería (Molina-Sanchis et al., 2016), Murcia (Amengual et al., 2015; Conesa- García et al., 2017; Hooke, 2016), Almería and Murcia (Bracken et al., 2008), Alicante (Martínez-Ibarra, 2012; Olcina-Cantos et al., 2010), Murcia and Alicante (Pérez- Morales et al., 2015), Valencia (Camarasa-Belmonte, 2016; Camarasa-Belmonte et al., 2011; Camarasa-Belmonte and Segura-Beltran, 2001) and Barcelona (Ballesteros et al., 2018). Nevertheless, the study of temporal evolution of hydrological response as a consequence of land use changes along time has not yet fully undertaken jointly with high intensity convective storms.

In order to predict flash floods events and their variations due to land use changes, the Soil and Water Assessment Tool (SWAT) was employed (Arnold et al., 1998; Neitsch et al., 2011; Winchell et al., 2013). It presents the following advantages: i) Currently, few numerical models calculate hydrological processes at watershed scale with sub-daily time steps, required to correctly simulated the hydrological response of short-time concentration basins (Boithias et al., 2017; Jeong et al., 2010; Li et al., 2018; Rozalis et al., 2010; Yang et al., 2015). This temporal resolution is essential to capture the hydrologic complexity of flash floods events. ii) SWAT reaches spatial accuracies at hydrological response unit (HRU) being suitable to assess the land use influence into the results of the present study. iii) The SWAT model has been widely applied in ungauged basins obtaining, generally, good results (Boongaling et al., 2018; Gassman et al., 2007; Gassman et al., 2014). This is important because ravine basins in the study area do not show gauge stations due to the intermittent water flow regime. Scientific literature reports robust uncalibrated models with appropriate results in ungauged basins. Even, in semi-arid regions, some experiences showed uncalibrated and calibrated models with similar results (Beven, 1989; Lange et al., 1999; Miao et al., 2016; Michaud and Sorooshian, 1994; Michaud et al., 2001; Perrin et al., 2001; Rozalis et al., 2010; Silvestro et al., 2017).

The aim of the study is to analyse the temporal evolution of the discharge rates as a consequence of changes in cover land uses, essentially due to tourism and urban growth. Five ravine basins (*San Juan*, *Juncaret*, *Alicante Puerto*, *Oveja* and *Agua Amarga*) located in the Alicante province and representing typical fluvial systems of Mediterranean semi-arid environments with ephemeral streams, moderately steep slopes, short concentration times and with registered critical flash floods episodes during last decades were selected.

To get this objective, first, the runoff curve number was calculated at a HRU spatial resolution. Second, design storms were generated for each basin independently, according to their time of concentration. And third, the watershed response to these storms was achieved using the SWAT model with a sub-daily time step. These procedures were accomplished with five land use scenarios in order to assess the impact of urban development in the studied catchments. Finally, Kruskal-Wallis and post-hoc statistical tests based on Mann-Whitney test

with BH correction (Benjamini and Hochberg, 1995; Kruskal and Wallis, 1952; Sheskin, 2007) were performed to evaluate the changes significance obtained in the discharge rates.

2. Study area

This project is focused in the semi-arid domain of the Alicante province (SE Spain). The region has a semi-arid Mediterranean climate with mean annual temperature of 18 °C, and low total annual precipitation values, ranging from 250 to 350 mm/year in the selected basins. Precipitation is unevenly distributed along the year, with dry summers and autumns concentrating the majority of precipitation. Climatic data was obtained from daily temporal series provided by the Spanish National Meteorological Agency (AEMET, 2018). Very important precipitation events are common in autumn and episodes of more than 200 mm in one day have been registered (Martínez-Ibarra, 2012; Valdes-Abellan et al., 2017).

The selected study ravine basins are *San Juan*, *Juncaret*, *Alicante Puerto*, *Oveja* and *Agua Amarga*. They all five are fluvial systems that drain to the coastline of the Alicante municipality (Fig. 1). These Mediterranean catchments present different sizes, with areas ranging from 10.2 km^2 to 200.9 km^2, moderately steep slopes and ephemeral streams (Table 1), according to the digital elevation model (DEM) available in *Centro Nacional de Información Geográfica* (CNIG, 2017). Characteristic orography, with elevations up to 1400 m in less than 20 km from the coastline, produces rainfall water concentrates rapidly increasing flash floods risk (Martínez-Ibarra, 2012; Valdes-Abellan et al., 2017).

Study watersheds are situated in the eastern part of the Baetic mountain range (Prebaetic System). They are characterised by a certain lithological diversity with materials from the Tertiary, Jurassic and Quaternary periods (DPA-IGME, 2015). Regarding their geomorphology, landforms are dominated by gravels, sands, clays and silts from glacis and foothills deposits, with some inclusions of sandstones and limestones (IGME, 2018). Data from the Harmonized World Soil Database (HWSD, 2017) denote that haplic calcisols, calcaric cambisols and haplic gypsisols are the dominant soil classes (Table 1).

At present time, Alicante province is the fifth most populated region in Spain with 1,825,332 inhabitants; 59.3 % of them are located in coastal municipalities. In addition, the

touristic activity attracts more than 3.4 million tourists and 14.5 million overnight stays per year, mainly concentrated in summer (INE, 2017; Sánchez-Galiano et al., 2017). Alicante municipality, where the outlets of all selected basins are located, is the most populated in the province, with 330,525 inhabitants (INE, 2017). Jointly with this demographic development, urban areas have largely increased during last four decades mainly in the coastline and often without a suitable urban development plan (Olcina-Cantos et al., 2010; Pérez-Morales et al., 2015). Consequently, some of these basins have approximately 70 % of their surface occupied by urban areas (Table 1) with high population density according to the Corine Land Cover (CLC) database (CNIG, 2017).

The risk associated to flash floods increases as a consequence of the combination of high intensity precipitation threat and vulnerable land uses. In addition, this situation even affects to the sediment transport toward the coast due to large terrain waterproofing rates (Pagán et al., 2018). Local authorities, within a flood risk prevention plan (PATRICOVA, 2015), are trying to reduce flash floods effects by, among others, hydraulic infrastructures as the floodable park *La Marjal* and the *José Manuel Obrero Díez* tank, placed respectively in *San Juan* and *Alicante Puerto* ravine basins. However, these hydraulic barriers were insufficient against the last flash floods events, in December 2016 and March 2017, with two human deaths and very severe economic impacts (Jodar-Abellan et al., 2018; Morote-Seguido and Hernández-Hernández, 2017).

3. Methodology

Hydrological simulations have been accomplished with SWAT (Neitsch et al., 2011), a semi-distributed, time-continuous hydrological tool at basin scale. It is a physically based model which can be applied to a wide range of cases such as climate change impacts on water resources (Ashraf-Vaghefi et al., 2013; Faramarzi et al., 2013), land-management practices on water (Abbaspour et al., 2015), sediment transport and agricultural chemical yields in gauged and ungauged watersheds (Azimi et al., 2013; Rouholahnejad et al., 2014) or microbial contamination and fate from dairy farms (Arnold et al., 1998; Arnold et al., 2012; Gassman et al., 2007; Gassman et al., 2014; Park et al., 2016). Recent improvements in the model time

resolution allow simulating with time steps of minutes, placing SWAT as a suitable tool to accomplish flash floods studies (Boithias et al., 2017; Jeong et al., 2010).

3.1. Cover data and land use scenarios

Basins and subbasins were delineated based on a DEM with a spatial resolution of 25 m x 25 m (CNIG, 2017). In line with Tarboton et al. (1991), DEM was pre-filtered using GIS tools to remove sinks and peaks, ensuring a later proper delineation of watersheds, subbasins and streams and avoiding the generation of discontinuous drainage systems. To improve the mentioned delineation, the drainage network layer, scale 1:25,000, modified from the Pfafstetter national river classification (MAPAMA, 2017) was also used. The basin output in all basins was fixed next to the Mediterranean Sea.

The generated subbasins were subdivided into hydrological response units (HRUs) with homogeneous land use, slope, and soil features (Neitsch et al., 2011). Therefore, a raster cover data of soils, with a scale of 1:1,000,000, was used (HWSD, 2017). The soil codes from HWSD (2017) were adapted and included into the SWAT2012 database. Slope was divided into two classes (0%-3% and >3%) following the 5.2-IC Spanish normative (BOE, 2016). Land use data was obtained from CLC database with a scale of 1:100,000 (CNIG, 2017). A baseline scenario with no urban land use and CLC data from 1990, 2000, 2006 and 2012 were considered yielding five scenarios: baseline, CLC1990, CLC2000, CLC2006 and CLC2012. Similarly to Pulido-Velazquez et al. (2015), the baseline scenario was generated using the CLC1990 and assigning proportionality agricultural and natural land use classes to urban classes. Land uses from CLC were reclassified into SWAT land use classes following Dunea et al. (2016), El-Sadek and Irvem (2014), Koulov and Zhelezov (2016), Koutalakis et al. (2001) and Koutalakis et al. (2015). These reclassifications are shown in Table 2.

The runoff curve number for moisture condition II (CN2), attending to the Soil Conservation Service (SCS, 1986) nomenclature, and the average sub-daily streamflow out of each subbasin (flow_out) were selected using the sub-daily SWAT model (Jeong et al., 2010; Winchell et al., 2013), version 2012.10.2.18, as a coupled extension to ArcGIS tool

(ArcSWAT). Finally, the obtained CN2 was modified according to the slopes in each HRU using the Williams (1995) method.

*3.2. Design storms and meteorological data*Time of concentration (*Tc*) for each basin was calculated using the empirical equations developed by Neitsch et al. (2011) considering main and tributary channels at a subbasin level. The *Tc* of each watershed was accomplished selecting subbasins which main and tributary channels define the longest water routing. A *Tc* of 1.57 hours was obtained in the *San Juan* ravine basin, 2.41 hours in *Juncaret*, 1.93 hours in *Alicante Puerto*, 4.59 hours in *Oveja* and 2.76 hours in *Agua Amarga* (Table 1).

Next, the Intensity-Duration-Frequency (IDF) function (Eq. (1)) was obtained for the observed meteorological data in the the 8025 station (Koutsoyiannis et al., 1998):

$$I = \frac{a \cdot T^{n}}{(T_c + b)^{m}} \quad (1)$$

where I is the intensity (mm/hours); T is the return period (years); Tc is the time of concentration (hours); a, n, b and m are specific coefficients for the 8025 station. The selected meteorological station presents the longest daily registers (from 1921) and the lowest presence of gaps. Later, synthetic rainfall events were obtained for each basin following the non-symmetric alternating blocks method (Chow et al., 1988). Fig. 2 shows the synthetic rainfalls intensities generated to each ravine basin considering a return period of 100 years and a time step of 10 minutes.

SWAT also requires daily meteorological series of maximum and minimum temperatures (*Tmax* and *Tmin*), relative humidity, solar radiation and wind speed (Winchell et al., 2013). Daily registers of *Tmax* and *Tmin* were obtained from the 8010A, 8014I, 8019, 8021A, 8025, 8025A and 8026A meteorological stations (AEMET, 2018) and used in each watershed according to their proximity (Fig.1). These stations were selected on account of temporal lengths for meteorological data of 30 years or more. Potential evapotranspiration was simulated with the Hargreaves et al. (1985) method. Daily series of relative humidity, solar radiation and wind speed were obtained using the weather generator of the SWAT model (Neitsch et al.,

2011; Sharpley and Williams, 1990). Meteorological parameters with a monthly time level, needed to run this generator, were calculated using data from the ALC20wgn station (Fig.1).

3.3. Surface runoff, flood propagation and velocity of flow

Rainfall-runoff conversion was accomplished through the Green and Ampt infiltration method (Green and Ampt, 1911), lately modified by Mein and Larson (1973). The Green-Ampt Mein-Larson excess rainfall method, coupled in SWAT by Jeong et al. (2010), is considered appropriated to achieve the objectives of the present study because of the requirement of sub-daily precipitation data and the inclusion of the curve number variations (land cover impacts) into the effective hydraulic conductivity expression (Bauwe et al., 2017; Boithias et al., 2017; Jeong et al., 2010; Maharjan et al., 2013; Nearing et al., 1996; Neitsch et al., 2011). Flood propagation in channels was simulated using the Muskingum river routing method (Cunge, 1969; Overton, 1966) whose main expression is presented in Eq. (2):

$$V_{stored} = K \cdot (X \cdot q_{in} + (1 - X) \cdot q_{out}) \quad (2)$$

where V_{stored} is the storage volume (m^3 H_2O); K is the storage time constant for the reach segment (s); q_{in} is the inflow rate (m^3/s); q_{out} is the discharge rate (m^3/s); and X is a weighting factor that regulates the relative importance of q_{in} and q_{out} into the reach storage. According to Neitsch et al. (2011), a X of 0.2 was assigned in the watersheds channels. Regarding K, it depends on two calibration coefficients that control the impact of high flow (K_{co1}) and low flow (K_{co2}) in the propagation process. Values of 0.25 for K_{co1} and 0.75 for K_{co2} were used in this study attending to the channel characteristics of the catchments and the experiences of Cunge (1969) and Overton (1966).

Manning's equation for uniform flow (Manning et al., 1977) was considered to calculate the rate and velocity of water in the overland and in the main and tributary channels (Eq. (3) and Eq. (4)):

$$v_{ov} = \frac{0.005 \cdot {L_{slp}}^{0.4} \cdot slp^{0.3}}{{n_{ov}}^{0.6}} \quad (3)$$

$$v_c = \frac{0.317 \cdot Area^{0.125} \cdot {slp_{ch}}^{0.375}}{{n_c}^{0.75}} \quad (4)$$

where v_{ov} is the overland flow velocity (m/s); L_{slp} is the subbasin slope length (m); *slp* is the average slope in the subbasin (m/m); and n_{ov} is the Manning's roughness coefficient for the subbasin. v_c is the average channel velocity (m/s); *Area* is the subbasin area (km^2); slp_{ch} is the channel slope (m/m); and n_c is the Manning coefficient for the channel. In this study, n_{ov} values were assigned according to the land use classes (Table 2) following the Engman (1986) categories. Regarding n_c, two coefficients were chosen based on the basins knowledge and Kehew et al. (2010) experiences. A coefficient of 0.021 corresponding to the channel category of "Excavated or dredged/Earth, straight and uniform" in Chow (1959) was given to the main and tributary channels located in urban subbasins. However, channels in subbasins with natural or agricultural land use received a coefficient of 0.065 corresponding to "Natural streams/Few trees, stones or brush" (Chow, 1959; Kehew et al., 2010).

Both Manning and Muskingum methods reported good results in certain experiences performed in arid and semi-arid Mediterranean areas using SWAT (Kehew et al., 2010).

*3.4. Water flow in urban areas*SWAT classifies urban use in four categories: pervious and impervious areas hydraulically connected or not to the drainage system. These considerations allow obtaining an increase in the total runoff volume, flow velocity and peak flood discharges typical of urban areas (Neitsch et al., 2011). Thus, surface runoff calculations require a corrected curve number (Eq. (5) and Eq. (6)):

$$CN_c = CN_p + imp_{tot} \cdot \left(CN_{imp} - CN_p\right) \cdot \left(1 - \frac{imp_{dcon}}{2 \cdot imp_{tot}}\right) \quad if\ imp_{tot} < 0.30 \quad (5)$$

$$CN_c = CN_p + imp_{tot} \cdot \left(CN_{imp} - CN_p\right) \quad if\ imp_{tot} > 0.30 \quad (6)$$

where CN_c is the corrected runoff curve number for moisture condition II (CN2); *CNp* is the initial CN2 in pervious areas; CN_{imp} is the CN2 for impervious areas; imp_{tot} is the fraction of the HRU that is impervious (both directly connected and disconnected); and imp_{dcon} is the fraction of the HRU that is impervious but not hydraulically connected to the drainage system (Arnold et al., 2012; Neitsch et al., 2011; SCS, 1986). In urban areas, the implemented version of the SWAT tool assigns the same *CNp* values into the four Hydrologic Soil Groups omitting the differences between urban classes (*CNpA:*31; *CNpB:*59; *CNpC:*72; and *CNpD:*79). In this work,

according to the study area knowledge and the *CNp* categories stablished in SCS (1986), different *CNpA, CNpB, CNpC* and *CNpD* values were assigned to each urban area into the SWAT database. CN_{imp} was considered equal to 98 in all urban areas while Imp_{tot} and imp_{dcon} were modified at a HRU level (Neitsch et al., 2011). Finally, the obtained *CNc* is later modified according to the slope in the same way as in non-urban areas.

Simulation in urban areas used the Buildup/Wash Off algorithm. This algorithm, similar to the Storm Water Management Model, divides each HRU into pervious and impervious areas (Arnold et al., 2012; Huber and Dickinson, 1988). The algorithm affects peak runoff rate calculation (mm/hr) mainly with a wash off coefficient (mm^{-1}) that received a 0.19 value in urban areas (Huber and Dickinson, 1988; Sonnen, 1980). *3.5. Setup the SWAT sub-daily model*

SWAT tool was run with a time step of 10 minutes using the sub-daily runoff module of the model. The 10-minutes time step is appropriate to represent the characteristic and quick development of flash floods events; satisfactory results with this time step were provided King (2000) using the Green and Ampt equation. Detail information about the sub-daily SWAT module and further modifications can be found in Arnold et al. (2012), Bauwe et al. (2017), Boithias et al. (2017), Jeong et al. (2010), Maharjan et al. (2013), Neitsch et al. (2011) and Yang et al. (2015), among others.

3.6 Hydrologic parameters regionalisation

Study watersheds do not possess gauge stations with reliable streamflow series as can be verified in national Spanish networks (CEDEX, 2018; ROEA, 2018; SAIH, 2018; SIA, 2018) and regional sub-networks (CHJ, 2018; DPA-IGME, 2015). Therefore, traditional sensitive analysis and the subsequent uncertainly analysis (calibration and validation) to correct initial values of hydrologic parameters through stream gauge series (inverse modeling: Abbaspour et al., 2015), was inviable. Nevertheless, the hydrological model intricacy, required in flash flood simulations, has been analysed in detail (Miao et al., 2016; Michaud and Sorooshian, 1994;

Michaud et al., 2001). In floods modeling, a long set of parameters could rises the prediction uncertainty. Thus, to reduce this uncertainty, extend calibration processes are required (Beven, 1989; Perrin et al., 2001). At the same time, robust uncalibrated models reported appropriate results in ungauged basins. Even, in semi-arid regions, some experiences showed uncalibrated and calibrated models with similar results (Gaume et al., 2010; Lange et al., 1999; Miao et al., 2016; Michaud and Sorooshian, 1994; Nguyen et al., 2014; Rozalis et al., 2010; Silvestro et al., 2017).

Considering previous issues, and keeping in mind that the main objective of the present study is assessing relative changes in discharge rates due to land use changes, certain regionalized parameters were adopted from Gomariz-Castillo (2016), and Gomariz-Castillo and Alonso-Sarría (2018). Both works were performed in two watersheds in the Alicante province, that surround the studied ravine basins: the Vinalopó river watershed in the South and the Monnegre river watershed in the North. These catchments present similar features to the assessed basins (steep slopes, land uses, soils, high rainfall intensities, etc.) and were calibrated and validated using the SIA (2018) Spanish network. Finally, obtained results in the five basins of the present work were checked (validated) with several technical studies developed in the studied and contiguous areas within the framework of a relevant flood risk prevention plan (PATRICOVA, 2015) from the Alicante, Valencia and Castellón provinces.

3.7. Statistical analysis between the different scenarios

Results of the storm hydrographs (streamflow), obtained at the mouth of the basins, in the coastline, were statistically treated to capture hydrological processes differences derived from the implemented land use scenarios (baseline, CLC1990, CLC2000, CLC2006 and CLC2012). Firstly, the null hypothesis of hydrographs equality was tested. All discharges data were also verified for normality using the Lilliefore test and for homoscedasticity through the Levene's test. Although homoscedasticity tests were not significant, Lilliefore tests indicated non-normality. Therefore, the Kruskal-Wallis ANOVA analysis was implemented (Kruskal and Wallis, 1952). Detail information about this statistical contrast and its development can be found in Sheskin (2007). This test, that uses the ranks of the data values, is the non-parametric

alternative to the one-way analysis of variance (one-way ANOVA). Thus, in the Kruskal-Wallis ANOVA analysis, the statistical test is compared to a critical Chi-squared (X^2) theoretical value for a given confidence level (α= 0.05 in the present study). Hence, p-value < α (significant test) can be considered as a significant difference among the discharge values.

When significant differences between scenarios were observed, a post-hoc contrast among pairs of scenarios based on Mann-Whitney, and using BH method (Benjamini and Hochberg, 1995) to correct p-values between scenarios, was performed in order to discover groups of non-significantly different scenarios. All the statistical analysis were achieved with R-CRAN (2018).

4. Results and discussion

4.1. Land use changes

Land use classes are classified into three general categories (Table 3). Urban category contains the URLD, URML, URHD, UTRN, UCOM and UIDU land use codes. Likewise, agricultural group includes the AGRL, AGRC, AGRR, GRAP, ORCD, OLIV and PAST codes. Finally, natural category encloses the FRSE, RNGE, RNGB, SWRN, BARR and WATR codes. A detail description about these codes and their land use classes is presented in Table 2.

On the one hand, the five ravine basins increased highly their urban areas: currently, *Juncaret*, *San Juan* and *Alicante Puerto* basins are the three fluvial systems with the highest percentage of urban areas reaching 75% in the last two cases. Meanwhile, *Agua Amarga* and *Oveja* basins show, respectively, a 9.3% and a 15% occupied by urban land use (Table 3). Along time, a general change in the urban land use classes is also observed: initial scenarios (1990 and 2000) showed mainly urban areas with low and medium population density (URLD and URML respectively), while current scenarios (2006 and 2012) present urban areas with a clear demographic density increase (URHD). A good example is identified in the *Alicante Puerto* basin that presented a 24.5% of URHD in 1990 and a 31.8% of its total surface occupied by this class in 2006. In addition, latest scenarios show a considerable rise of their commercial, transportation and industrial areas (UCOM, UTRN and UIDU respectively) as depicted in Fig. 3c. These changes in the urban land use classes are consistent with the urban growth and the high demographic pressure described in Ballesteros et al. (2018), Camarasa-Belmonte et al.

(2011), Conesa-García et al. (2017), etc. along the Southeast coast of Spain during last years and, specially, in the coastline of the Alicante and Murcia provinces (Pérez- Morales et al., 2015).

On the other hand, an important decrease in agricultural land use was detected over the studied period (1990-2012, Table 3). *Agua Amarga* lost 17.4 km^2 (-36.9%) of agricultural land use; *Oveja* presents a decrease of 58.3 km^2 (-51.5%); *Alicante Puerto* shows a reduction of 5.4 km^2 (-51.9%); *Juncaret* misplaced 24.8 km^2 (-54.7%); and *San Juan* presents a reduction of 5.1 km^2 (-68.9%). According to recent studies performed in the SE of Spain (Alonso-Sarría et al., 2016; García-Ruiz and Lana-Renault, 2011; Rodrigo-Comino et al., 2018), the observed abandonment of agricultural areas was due to environmental factors related, mainly, to climate, pedology and topographic limitations (e.g., intensification in the occurrence of small landslides) and by numerous socio-economic factors derived from European Agricultural Policies, unsuitable intensive uses of the land, and so one. Additionally, the studied catchments suffered several conversions from cover areas into urban zones (Fig. 3a and c).

Agricultural land use was dominated by complex cultivation patterns (AGRR) and land principally occupied by agriculture, with significant areas of natural vegetation (AGRL). These classes showed low alterations during the studied periods. However, 1990 and 2000 scenarios exhibited numerous areas with fruit trees and berry plantations (ORCD) and vineyards (GRAP) which reduced their surfaces considerably in 2012. At the same time, an important increase of pastures (PAST) was observed in 2012 (Fig. 3a and c) as the class where abandoned areas moved first. These findings are in agreement with the experiences of Garcia-Diaz et al. (2018) and García-Ruiz and Lana-Renault (2011) developed in the Southeast of Spain.

Natural areas of the *Agua Amarga*, *Oveja* and *Juncaret* catchments raised greatly during the studied periods, principally, due to the mentioned agricultural abandonment. However, in *Alicante Puerto* and *San Juan* basins this category is scarce (Table 3). In the five watersheds, natural grassland (RNGE) and sclerophyllous vegetation (SWRN) are the main natural land uses throughout the 1990-2012 period, without considerable changes between scenarios. Likewise, an enlargement in transitional woodland-shrub (RNGB) and forest (FRSE) was identified in the

latest scenarios (Fig. 3a and c). Similar trustworthy results were also achieved in Garcia-Diaz et al. (2018) and Romero-Díaz et al. (2017).

4.2. Curve number II variations

Observed curve number (CN2) variations among scenarios were due exclusively to changes in land uses since all other factors (slope and hydrologic soil groups) remained equal along the analysed period in the study area. Fig. 3 shows the two scenarios with the biggest differences between them (baseline and 2012). Specially relevant are the urban land uses which produce great increases in CN2 levels as can be observed in residential-high density (URHD), transportation (UTRN) and industrial (UIDU) classes with CN2 varying from 87.5 to 92.5 (Fig. 3c and d). Therefore, in these areas around 90% of the precipitation is converted to surface runoff and only 10% would percolate into soil layers. This great terrain waterproofing rate increases highly the risk of flooding. In Alicante province as it will be shown in the following section, the increment in the flood hazard due to urban areas was highlighted by Martínez-Ibarra (2012), Olcina-Cantos et al. (2010) and Pérez-Morales et al. (2015), among others. Meanwhile, agricultural and natural areas of the studied basins presented reductions in the obtained CN2 as a consequence of their limited impermeable surface, even when they are located in areas (normally the headwater and medium subbasins) with average slopes higher than the registered in urban areas, usually placed in the flatter coastline (Fig. 3).

An aggregate analysis is presented in Table 3 to show the great differences identified in CN2 levels of urban, agricultural and natural areas. This table includes the five studied scenarios and the CN2 values of each land use category. Thus, in the five ravine basins, urban category experimented gradual increases from 1990 to 2012 with CN2 levels varying, respectively, from 81 to 89 (Table 3). These rises in CN2, among scenarios, are due to the recognized growth of urban areas with high population density, transportation and industrial classes within the study period. Special attention requires *San Juan* catchment which presented the highest CN2 value (86.6) in scenario 1990 because of the absence of urban areas with low population density (URLD). However, in the remaining scenarios (2000, 2006 and 2012) some residential areas spread, with parks and green zones, occupying around 3.2% and 4.4% of the watershed.

Consequently, aggregated CN2 values, depicted in Table 3, went down moderately in the 2000, 2006 and 2012 scenarios.

Regarding agricultural areas, CN2 ranges from 52 to 64 (Table 3). Between scenarios, CN2 did not show considerable changes, because there were low variations in their most extended land uses classes (AGRR and AGRL) within the study period. In particular, *Juncaret* and *San Juan* basins achieved CN2 values (around 60) discreetly higher than the registered in the other watersheds. Since both catchments did not reach large variations in their land use classes regarding the other ravine basins, neither steeper average slopes (Table 1), it is considered that their main soil class (calcaric cambisols with inclusions of chromic luvisols) explains these moderately higher CN2 values in the studied scenarios (Table 3). Detail analysis, developed in the five watersheds, reported that the mentioned soil class usually presents numerous clay deposits, increasing its terrain waterproofing rates and being classified as Hydrologic Soil Group type C (HWSD, 2017; IGME, 2018; SCS, 1986).

Natural areas achieved CN2 varying from 42 to 60 and it is the category with the lowest CN2 average values (Table 3). In general, CN2 obtained increases moderately among scenarios (from 1990 to 2012) which are related to the different permeability of the main land use classes recognized in each period (RNGE, SWRN, RNGB and FRSE). Finally, individual analysis performed in each scenario of the five watersheds, showed that land use is the variable with the highest impact on CN2, followed by the average slope. This close relation among land use and CN2 has been widely assessed in scientist literature (Amengual et al., 2015; Bauwe et al., 2017; Boongaling et al., 2018; Rozalis et al., 2010).

4.3. Temporal and spatial discharges changes

Land use changes and specially the great urban growth identified in the study area produced basins answering with high discharge rates to the five design storms, representative of Mediterranean convective systems. Figure 4 depicts the hydrographs for each scenario obtained at the outlet of the lowest and highest subbasin.

Storm hydrographs of the headwater subbasins presented variations among scenarios, mainly, due to the impact of different overland Manning's roughness (n_{ov}) from each land use

class (Table 2) to the amount and water velocity (Eq. (3)). In the case of *Oveja*, *Juncaret* and *Agua Amarga* basins discharge differences were caused by agricultural and natural land use changes since no urban development was observed in those subbasins. For example, *Agua Amarga* headwater registered in the baseline and 1990 scenarios peak runoff rates around 9.3 m^3/s being their main land uses ORCD (n_{ov}=0.6) and RNGE (n_{ov}=0.24). In 2000 and 2006 scenarios, peak runoff reached 11.6 m^3/s (Fig. 4e) because considerable increases of the RNGE land use were observed occupying 70% of the terrain in this subbasin. Finally, in 2012 peak flow achieved 13.1 m^3/s and RNGE use increased 81.4% of the subbasin area. Likewise, specifically relevant was the analysis in *Juncaret* headwater because in 2012 agricultural land use was replaced in numerous areas by natural land use, with higher n_{ov}. Therefore, a reduction of 7.5 m^3/s and a translation time of 0.5 hours were identified in the peak runoff rate regarding previous scenarios hydrographs (Fig. 4b). Similar trustworthy relations between overland Manning's roughness and discharge rates were achieved in *San Juan* and *Alicante Puerto* headwaters which were also affected by the great urban development described from 1990 to 2012 (Table 3). Thus, the different Manning's coefficients (n_c) of the main and tributary channels of urban areas (n_c=0.021) and the other two categories (n_c=0.065) produced large differences among storms hydrographs (Fig. 4a and c).

Hydrographs in the basins mouth, in the coastline, showed a clear impact by the land use changes that can be summarized as a general trend in all five basins as a reduction in the rising limb times and an increase in the peak discharge value (Fig. 4). The relative reduction in the rising limb time depends on the basin area. However, following a general rule, the higher the area the higher the reduction in the rising limb time, changing from 5 to 3 hours in *Alicante Puerto* and from 9 to 4 in *Agua Amarga* when comparing the first and last scenarios. For example, *Oveja* basin registered peak discharge of 60-63 m^3/s in the headwater subbasin after 4.6 hours from the beginning of the storm, while in the outlet, the peak discharge was achieved at 10.8 hours in the baseline scenario; at 7.5 hours in 1990; at 6.1 hours in 2000; at 5.8 hours in 2006; and, finally, at 5.5 hours in 2012 (Fig. 4d). Special attention requires the *Alicante Puerto* basin in the 1990 scenario (Fig. 4c) because the peak runoff rate was reached at 4.6 hours in the

headwater subbasin, whereas, in the outlet, maximum discharge was obtained at 3.1 hours. This singular situation was a consequence of several factors: in SWAT all subbasins receive precipitation to simulate properly the presence of several convective clouds (Arnold et al., 2012; Neitsch et al., 2011); and the outlet subbasin in *Alicante Puerto* presented small size (2.8 km^2) with extensive urban areas, while the headwater subbasin extension (13.8 km^2) was occupied, in 1990, by an important percentage of agricultural and natural areas (with high n_{ov}). Therefore, slower flood propagation was obtained in this headwater subbasin.

Spatial analysis confirmed the correct flood propagation among subbasins groups, validating the Muskingum river routing model as a reliable method to simulate water routing through the channels network. In addition, certain experiences accomplished in arid and semi-arid Mediterranean areas reached good results using the Muskingum method (Amengual et al., 2015; Kehew et al., 2010). Finally, it is worthy to consider that reductions in the rising limb time are critical when dealing with risk management in a society because the reduced time to organize emergency activities leads to a worse answer to a flood event and to more severe socio-economic impacts as a consequence of a specific rainstorm.

Regarding the peak discharge value, the most important changes are located mainly during the last decades of the XX century. As a general rule, differences between the 1990 scenario and the baseline are smaller than differences between 1990 scenario and the latest scenarios (Fig. 4). Compared to peak discharge values of 1990 scenarios (not considering the baseline results) peak discharge values in the last scenario roughly doubled in *Juncaret* and *Agua Amarga* basins (Fig. 4b and e), and multiplied its value by a factor larger than two in *San Juan*, *Alicante Puerto* and *Oveja* (Fig. 4a, c and d).

Fig. 5 depicts the two scenarios with the highest discharge differences between them (baseline and 2012). The peak runoff rates achieved in the coastline outlet in the baseline and CLC2012 scenarios were respectively: 105.1 m^3/s and 216.7 m^3/s for *Agua Amarga*; 378.4 m^3/s and 938.1 m^3/s for *Oveja*; 50.3 m^3/s and 234.3 m^3/s for *Alicante Puerto*; 190.5 m^3/s and 385.9 m^3/s for *Juncaret*; 27.5 m^3/s and 126.6 m^3/s for *San Juan*. Bronstert et al. (2018) and Scorpio et al. (2018) estimated approximate peak discharges in 11 catchments with similar features to the

assessed in this work, as their surfaces, cumulative rainfalls (60-360 mm in 12 hours), recurrence intervals of 100-150 years, etc. In addition, the obtained results are consistent with several technical studies performed in Alicante province within the Action Plan on Flood Risk Prevention (PATRICOVA in Spanish) developed since 2003 (PATRICOVA, 2015). One should consider if the infrastructures were designed to absorb the high increase in the discharge rates values produced as a consequence of the observed changes in land uses.*4.4 Streamflow statistical differences*

Discharge rates achieved at the basin mouths, in the coastline, were evaluated to capture statistical effects caused by the land use changes of the baseline, CLC1990, CLC2000, CLC2006 and CLC2012 scenarios. Results show significant differences in the *Alicante Puerto*, *Juncaret* and *San Juan* storm hydrographs (p-value < 0.0001; Table 4). This result denotes that subbasin outlets, from these watersheds, reached high and sudden streamflow modifications among land use scenarios. In particular, the greatest changes were obtained in the *Alicante Puerto* ravine basin ($X^2(4) = 83.35$, $p < 0.0001$). Meanwhile, the *Oveja* catchment presented the smallest variations ($X^2(4) = 5.36$, $p = 0.2517$; Table 4). *Oveja* and *Agua Amarga* watersheds presented some discharge differences (Fig. 6), but smaller than the achieved in the other basins. Hence, they were not identified as significant by the performed statistical contrast.

Detail variances among class pairs (land use scenarios), from each basin, were represented in Fig. 6 based on their mean and median. In general, gradual rises of the average streamflow (red points and red lines in Fig. 6) and median reductions (black points and black lines in Fig. 6) were reached from the baseline to the 2012 scenario. This determined an asymmetric distribution of streamflow values, with a bias oriented to the right, which increased progressively. These findings, together with the identified hydrograph dynamics (Fig. 4), showed a significant spread of peak runoff rates in the first hours from the storm beginning. Hence, sensible enlargements of the discharge ascending slope, higher concentration crests and recession curves characterised by a greater slope were recognized after the peak runoff (Fig. 4).

Regarding the post-hoc test based on Mann-Whitney using BH method (Benjamini and Hochberg, 1995) and $p < 0.05$, changes in letters “a”, “b”, “bc” and “c” represented groups of

significant different scenarios, being the "bc" letter a transitional (not significant) scenario (Fig. 6). Thus, in *San Juan* and *Alicante Puerto* ravine basins two groups with high changes were observed: baseline and 1990 scenarios in comparison to 2000, 2006 and 2012, showing statistical variances between them. In the case of *Juncaret* catchment, although a similar behaviour to previous basins was detected, median confidence intervals indicate significant modifications in 2012 with regard to other scenarios (Fig. 6).

Therefore, obtained statistical results are direct consequence of the urban growth identified in the studied watersheds (with further effects in curve number and discharge rates) due to the fact that most urbanized ravine basins, *Alicante Puerto* and *San Juan*, presented the highest statistical differences among land use scenarios.

5. Conclusion

The main conclusions extracted from the present work are listed below:

- The studied Mediterranean coastal watersheds (*San Juan*, *Juncaret*, *Alicante Puerto*, *Oveja* and *Agua Amarga*), located in the Alicante province (SE Spain), enhanced considerably their urban areas in the last 22 years (1990-2012) without following a sensible criterion in response to flood risk consequences. Some of them experimented urban land use increases that surpass 70%. Additionally, an important abandonment of agricultural zones was identified, in part, due to its conversion in urban land use.
- This poorly planned urban development, shaped by a great local population growth and a considerable touristic activity, derived in highly vulnerable situations and amplified the original flood hazard of these coast areas, generating curve number that reaches even 85 and 90 levels.
- Hydrological response of the study basins to the 100-year return period design storm shows a high variation among the five considered land use scenarios: baseline, 1990, 2000, 2006 and 2012. According to the performed statistical tests (Kruskal-Wallis and post-hoc contrasts based on Mann-Whitney test with BH correction), some peak runoff rates from subbasins outlets, in the coastline, showed significant differences from the baseline land use scenario (≈ 50 m^3/s, 190 m^3/s, 380 m^3/s) to the most urbanised

scenario (≈ 235 m^3/s, 385 m^3/s, 940 m^3/s respectively). Consequently, the risk of flash floods increased in the region by both a spread in the vulnerability and an enlargement in the expected flow discharges.

- Implemented sub-daily SWAT model and GIS-based tools have proved to be useful when performing the study objectives. Within the SWAT code, the Green-Ampt Mein-Larson model and the Muskingum method were suitable to resolve, respectively, the rainfall-runoff conversion and the flood propagation equations. Thus, introduced corrections in the urban areas curve numbers, and the channel and overland Manning equations, related with the flow velocity, together with the different Manning roughness coefficients chosen, were essential to translate the real land use categories of the study catchments into the SWAT model.
- The obtained results can help water management authorities in the decision-making process against flash flood effects, specially in the framework of the Action Plan on Flood Risk Prevention (PATRICOVA in Spanish) developed in the Alicante, Valencia and Castellón provinces since 2003. Results highlight the great urban development that may appear in coastal areas, and the subsequent necessity of considering future urban developments, even if they are not planned or expected at the time when flood risk prevention plans are being designed.
- Flash floods studies aiming to capture the high complexity (orographical and meteorological) of Mediterranean coastal catchments must continue to analyse population vulnerability and socio-environmental risk perception. Both of them are specially important in sensible areas of the SE of Spain which present extended urban areas into floodplains.
- Finally, this model will allow accomplishing further research in the evaluated watersheds related mainly with: 1-the recognized abandonment of agricultural areas, particularly important in headwater subbasins, and their expected influence into peak runoff rates; 2-several alterations of the sediment transport toward the coast due to large

terrain waterproofing rates as a consequence of the identified urban development; 3-an increase in the occurrence of high intensity storms as a consequence of climate change.

Acknowledgements

Financial support was provided partially by the University of Alicante, project GRE17-12. This study also has been conducted within the grant received from the *Programa Nacional de Formación de Profesorado Universitario* (FPU) conceded by the Spanish Ministry of Science to the first author. In the same way, the authors acknowledge the reviewers of the manuscript whose comments contributed greatly to improve this paper.

List of figures

Fig. 1. Study ravine basins.

Fig. 2. Design storms intensities calculated for each ravine basin.

Fig. 3. Curve number II variations, at hru level, considering land use coverages of the baseline and 2012 scenarios.

Fig. 4. Storm hydrographs, in the headwater and outlet subbasins, of the studied watersheds: *San Juan* (a), *Juncaret* (b), *Alicante Puerto* (c), *Oveja* (d) and *Agua Amarga* (e).

Fig. 5. Maximum discharge (m^3/s) spatial distribution, at subbasin scale, within the baseline (a) and 2012 (b) scenarios.

Fig. 6. Effect plots in watershed mouths, in the coastline, according to the considered land use scenarios. Black points and intervals represent the median and its confidence interval (95%). Red points depict its average streamflow. Letters indicate the obtained groups of significantly different scenarios (Mann-Whitney using BH method, $p < 0.05$) in median.

List of tables

Table 1

Main features of ravine basins.

Table 2

Corine Land Cover land use classes reclassified into SWAT land use classes (Baseline, 1990, 2000, 2006 and 2012 scenarios) and overland Manning's roughness coefficients according to the Engman (1986) categories.

Table 3

Weighted average curve number II dependent on main land use categories of the Baseline, 1990, 2000, 2006 and 2012 scenarios.

Table 4

Kruskal-Wallis ANOVA analysis of the storm hydrographs achieved at subbasin outlets in the coastline.

References

Abbaspour, K.C., Rouholahnejad, E., Vaghefi, S., Srinivasan, R., Yang, H., Klove, B., 2015. A continental-scale hydrology and water quality model for Europe: Calibration and uncertainty of a high-resolution large-scale SWAT model. Journal of Hydrology. 524, 733-752. https://doi.org/10.1016/j.jhydrol.2015.03.027.

AEMET, 2018. Registers of the Spanish National Meteorologial Agency (*Agencia Estatal de Meteorología*, AEMET). Alicante. (accessed 14 May 2018).

Alonso-Sarría, F., Martínez-Hernández, C., Romero-Díaz, A., Cánovas-García, F., Gomariz-Castillo, F., 2016. Main environmental features leading to recent land abandonment in Murcia region (Southeast Spain). Land Degradation & Development. 27, 654-670. https://doi.org/10.1002/ldr.2447.

Amengual, A., Homar, V., Jaume, O., 2015. Potential of a probabilistic hydrometeorological forecasting approach for the 28 September 2012 extreme flash flood in Murcia, Spain. Atmospheric Research. 166, 10-23. https://doi.org/10.1016/j.atmosres.2015.06.012.

Arnold, J.G., Kiniry, J.R., Srinivasan, R., Williams, J.R., Haney, E.B., Neitsch, S.L., 2012. Input/output documentation version 2012. Texas Water Resources Institute, Texas.

Arnold, J.G., Srinivasan, R., Muttiah, R.S., Williams, J.R., 1998. Large area hydrologic modeling and assessment part I: Model development1. JAWRA Journal of the American Water Resources Association. 34, 73-89. https://doi.org/10.1111/j.1752-1688.1998.tb05961.x.

Ashraf-Vaghefi, S., Mousavi, S.J., Abbaspour, K.C., Srinivasan, R., Yang, H., 2013. Analyses of the impact of climate change on water resources components, drought and wheat

yield in semiarid regions: Karkheh River Basin in Iran. Hydrological Processes. 28, 2018-2032. https://doi.org/10.1002/hyp.9747.

Azimi, M., Heshmati, Gh.A., Farahpour, M., Faramarzi, M., Abbaspour, K.C., 2013. Modeling the impact of rangeland management on forage production of sagebrush species in arid and semi-arid regions of Iran. Ecological Modelling. 250, 1-14. https://doi.org/10.1016/j.ecolmodel.2012.10.017.

Ballesteros, C., Jiménez, J.A., Viavattene, C., 2018. A multi-component flood risk assessment in the Maresme coast (NW Mediterranean). Natural Hazards. 90, 265-292. https://doi.org/10.1007/s11069-017-3042-9.

Bauwe, A., Tiedemann, S., Kahle, P., Lennartz, B., 2017. Does the Temporal Resolution of Precipitation Input Influence the Simulated Hydrological Components Employing the SWAT Model? Journal of the American Water Resources Association (JAWRA). 53, 997-1007. https://doi.org/10.1111/1752-1688.12560.

Benjamini, Y., Hochberg, Y., 1995. Controlling the false discovery rate: a practical and powerful approach to multiple testing. Journal of the Royal Statistical Society. Series B (Methodological). 57, 289-300. https://doi.org/10.2307/2346101.

Beven, K,. 1989. Changing ideas in hydrology-The case of physically-based models. Journal of Hydrology. 105, 157-172. https://doi.org/10.1016/0022-1694(89)90101-7.

BOE., 2016. *Proyecto de Orden Ministerial por la que se aprueba la Norma 5.2-IC Drenaje Superficial de la Instrucción de Carreteras. Boletín Oficial del Estado* (BOE). *Ministerio de Fomento*, Madrid.

Boithias, L., Sauvage, S., Lenica, A, Roux, H., Abbaspour, K.C., Larnier, K., Dartus, D., Sánchez-Pérez, J.M., 2017. Simulating flash floods at hourly time-step using the SWAT model. Water. 9, 1-25. https://doi.org/10.3390/w9120929.

Boongaling, C.G.K., Faustino-Eslava, D.V., Lansigan, F.P., 2018. Modeling land use change impacts on hydrology and the use of landscape metrics as tools for watershed management: The case of an ungauged catchment in the Philippines. Land Use Policy. 72, 116-128. https://doi.org/10.1016/j.landusepol.2017.12.042.

Bracken, L.J., Cox, N.J., Shannon, J., 2008. The relationship between rainfall inputs and flood generation in south-east Spain. Hydrological Processes. 22, 683-696. https://doi.org/10.1002/hyp.6641.

Bronstert, A., Agarwal, A., Boessenkool, B., Crisologo, I., Fischer, M., Heistermann, M., Köhn-Reich, L., López-Tarazón, J.A., Moran, T., Ozturk, U., Reinhardt-Imjela, C., Wendi, D., 2018. Forensic hydro-meteorological analysis of an extreme flash flood: The 2016-05-29 event in Braunsbach, SW Germany. Science of The Total Environment. 630, 977-991. https://doi.org/10.1016/j.scitotenv.2018.02.241.

Camarasa-Belmonte, A.M., 2016. Flash floods in Mediterranean ephemeral streams in Valencia region (Spain). Journal of Hydrology. 541, 99-115. https://doi.org/10.1016/j.jhydrol.2016.03.019.

Camarasa-Belmonte, A.M., López-García, M.J., Soriano-García, J., 2011. Mapping temporally-variable exposure to flooding in small Mediterranean basins using land-use indicators. Applied Geography. 31, 136-145. https://doi.org/10.1016/j.apgeog.2010.03.003.

Camarasa-Belmonte, A.M., Segura-Beltran, F., 2001. Flood events in Mediterranean ephemeral streams (ramblas) in Valencia region, Spain. Catena. 45, 229-249. https://doi.org/10.1016/S0341-8162(01)00146-1.

CEDEX, 2018. *Centro de Estudios y Experimentación de Obras Públicas*. http://www.cedex.es/CEDEX/lang_castellano/ (accessed 8 April 2018).

CHJ, 2018. *Confederación Hidrográfica del Júcar*. http://aps.chj.es/down/html/descargas.html (accessed 9 April 2018).

CNIG, 2017. *Centro Nacional de Información Geográfica*. http://centrodedescargas.cnig.es/CentroDescargas/index.jsp# (accessed 9 April 2018).

Conesa-García, C., García-Lorenzo, R., Pérez-Cutillas, P., 2017. Flood hazards at ford stream crossings on ephemeral channels (south-east coast of Spain). Hydrological Processes. 31, 731-749. https://doi.org/10.1002/hyp.11082.

Cunge, J.A., 1969. On the subject of a flood propagation computation method (Muskingum Method). Journal of Hydraulic Research. 7, 205-230. https://doi.org/10.1080/00221686909500264.

Chow, V.T., 1959. Open-channel hydraulics. McGraw-Hill, New York.

Chow, V.T., Maidment, D.R., Mays, L.W., 1988. Applied Hydrology. McGraw-Hill, Singapore.

DPA-IGME., 2015. *Atlas hidrogeológico de la provincia de Alicante: Excelentísima Diputación Provincial de Alicante* (DPA)-*Ciclo Hídrico. Instituto Geológico y Minero de España* (IGME). Alicante.

Dunea, D., Iordache, S., Dincă, N., Casadei, S., Petrescu, N., Nițu, I., 2016. Considerations regarding the agronomical variables associated to the performances of SWAT model simulations in the Romanian eco-climatic conditions. Agriculture and Agricultural Science Procedia 10. 5 th International Conference "Agriculture for Life, Life for Agriculture". 10, 83-93. https://doi.org/10.1016/j.aaspro.2016.09.020.

El-Sadek, A., Irvem, A., 2014. Evaluating the impact of land use uncertainty on the simulated streamflow and sediment yield of the Seyhan River basin using the SWAT model. Turkish Journal of Agriculture and Forestry. 38, 515-530. https://doi.org/10.3906/tar-1309-89.

Engman, E.T., 1986. Roughness coefficients for routing surface runoff. Journal of Irrigation and Drainage Engineering. 112, 39-53. https://doi.org/10.1061/(ASCE)0733-9437(1986)112:1(39).

Faramarzi, M., Abbaspour, K.C., Ashraf-Vaghefi, S., Reza-Farzaneh, M., Zehnder, A.J.B., Srinivasan, R.,Yang, H., 2013. Modeling impacts of climate change on freshwater availability in Africa. Journal of Hydrology. 480, 85-101. https://doi.org/10.1016/j.jhydrol.2012.12.016.

Garcia-Diaz, Y.P., Tenza-Abril, A.J., Pla, C., Valdes-Abellan, J., Jodar-Abellan, A., 2018. Land cover change dynamics in the Southeast of Spain. The abandonment of agricultural areas. EGU General Assembly. 20, Viena. Suiza.

García-Ruiz, J.M., Lana-Renault, N., 2011. Hydrological and erosive consequences of farmland abandonment in Europe, with special reference to the Mediterranean region-A review. Agriculture, Ecosystems and Environment. 140, 317-338. https://doi.org/10.1016/j.agee.2011.01.003.

Gassman, P.W., Reyes, M.R., Green, C.H., Arnold, J.G., 2007. The Soil and Water Assessment Tool: historical development, applications and future research directions. Transactions of the American Society of Agricultural and Biological Engineers (ASABE). 50, 1211-1250. https://doi.org/10.13031/2013.23637.

Gassman, P.W., Sadeghi, A.M., Srinivasan, R., 2014. Applications of the SWAT model special section: overview and insights. Journal of Environmental Quality. 43, 1-8. https://doi.org/10.2134/jeq2013.11.0466.

Gaume, E., Gaál, L., Viglione, A., Szolgay, J., Kohnová, S., Blöschl, G., 2010. Bayesian MCMC approach to regional flood frequency analyses involving extraordinary flood events at ungauged sites. Journal of Hydrology. 394, 101-117. https://doi.org/10.1016/j.jhydrol.2010.01.008.

Gomariz-Castillo, F., 2016. Estimación de variables y parámetros hidrológicos y análisis de su influencia sobre la modelización hidrológica: Aplicación a los modelos de Témez y Swat. Universidad de Murcia, Murcia.

Gomariz-Castillo, F., Alonso-Sarría, F., 2018. Efecto de la subdivisión de cuencas y la estimación de variables climáticas en la simulación hidrológica con el modelo SWAT en cuencas semiáridas mediterráneas. J.Exp. Psychol. Gen. 64, 1-20. https://doi.org/10.6018/geografia/2018/331531.

Green, W.H., Ampt, G.A., 1911. Studies on soil physics, 1. The flow of air and water through soils. The Journal of Agricultural Sciences. 4, 11-24. https://doi.org/10.1017/S0021859600001441.

Hargreaves, G.L., Hargreaves, G.H., Riley, J.P., 1985. Agricultural Benefits for Senegal River Basin. Journal of Irrigation and Drainage Engineering. 111, 113-124. https://doi.org/10.1061/(ASCE)0733-9437(1985)111:2(113).

Hooke, J.M., 2016. Geomorphological impacts of an extreme flood in SE Spain. Geomorphology. 263, 19-38. https://doi.org/10.1016/j.geomorph.2016.03.021.

Huber, W.C., Dickinson, R.E., 1988. Storm water management model, version 4: user's manual. Athens, Georgia.

HWSD, 2017. Harmonized World Soil Database. http://webarchive.iiasa.ac.at/Research/LUC/External-World-soil-database/HTML/ (accessed 14 March 2018).

IGME, 2018. Permeability Map of Spain in Shapefile format. Scale 1/200.000. *Instituto Geológico y Minero de España* (IGME). (accessed 19 March 2018).

INE, 2017. *Instituto Nacional de Estadística* (INE). https://www.ine.es/ (accessed 5 April 2018).

Jeong, J., Kannan, N., Arnold, J., Glick, R., Gosselink, L., Srinivasan, R., 2010. Development and integration of sub-hourly rainfall-runoff modeling capability within a watershed model. Water Resources Management. 24, 4505-4527. https://doi.org/10.1007/s11269-010-9670-4.

Jodar-Abellan, A., Melgarejo, J., Lopez-Ortiz, M.I., 2018. The floodable park "La Marjal" (Alicante, South East Spain) as a paradigmatic example of water reuse and circular economy, in: Syngellakis, S., Melgarejo, J., (Eds), WIT Transactions on The Built Environment., Southampton, UK, pp. 315-321. https://doi.org/10.2495/UG180291.

Kehew, A.E., Milewski, A., Soliman, F., 2010. Reconstructing an extreme flood from boulder transport and rainfall-runoff modelling: Wadi Isla, South Sinai, Egypt. Global and Planetary Change. 70, 64-75. https://doi.org/10.1016/j.gloplacha.2009.11.008.

King, K.W., 2000. Response of Green-Ampt Mein-Larsen simulated runoff volumes to temporally aggregated precipitation. Journal of the American Water Resources Association (JAWRA). 36, 791-797. https://doi.org/10.1111/j.1752-1688.2000.tb04306.x.

Koulov, G., Zhelezov, G., 2016. Sustainable mountain regions: challenges and perspectives in Southeastern Europe, Bulgaria. https://doi.org/10.1007/978-3-319-27905-3.

Koutalakis, P., Vlachopoulou, A., Zaimes, G.N., Loannou, K., Lakovoglou, V., 2001. Assessing soil erosion risk using USLE with GIS and SWAT for Thassos Island, Greece. 10 th International Congress of Hellenic Geographical Society. Greece.

Koutalakis, P., Zaimes, G.N., Emmanouloudis, D., Loannou, K., Lakovoglou, V., 2015. Using ArcSWAT to predict discharge in ungauge torrents of Thasos Island. 7 th International Conference on Information and Communication Technologies in Agriculture, Food and Environment (HAICTA), 154-162. Kavala, Greece.

Koutsoyiannis, D., Kozonis, D., Manetas, A., 1998. A mathematical framework for studying rainfall intensity-duration frequency relationships. Journal of Hydrology. 206, 118-135. https://doi.org/10.1016/S0022-1694(98)00097-3.

Kruskal, W.H., Wallis, W.A., 1952. Use of ranks in one-criterion variance analysis. Journal of the American Statistical Association. 47, 583-621. https://doi.org/10.2307/2280779.

Lange, J., Leibundgut, C., Greenbaum, N., Schick, A.P., 1999. A noncalibrated rainfall-runoff model for large, arid catchments. Water Resources Research. 35, 2161-2172. https://doi.org/10.1029/1999WR900038.

Li, D., Qu, S., Shi, P., Chen, X., Xue, F., Gou, J., Zhang, W., 2018. Development and Integration of Sub-Daily Flood Modelling Capability within the SWAT Model and a Comparison with XAJ Model. Water. 10, 1263-1280. https://doi.org/10.3390/w10091263.

Maharjan, G.R., Park, Y.S., Kim, N.W., Shin, D.S., Choi, J.W., Hyun, G.W., Jeon, J.H., Ok, Y.S., Lim, K.J., 2013. Evaluation of SWAT sub-daily runoff estimation at small agricultural watershed in Korea. Frontiers of Environmental Science & Engineering. 7, 109-119. https://doi.org/10.1007/s11783-012-0418-7.

Mahmood, M.I., Elagib, N.A., Horn, F., Saad, S.A.G., 2017. Lessons learned from Khartoum flash flood impacts: An integrated assessment. Science of the Total Environment. 601-602, 1031-1045. https://doi.org/10.1016/j.scitotenv.2017.05.260.

Manning, M.J., Sullivan, R.H., Kipp, T.M., 1977. Vol. III: Characterization of discharges. Nationwide evaluation of combined sewer overflows and urban stormwater discharges.

III. EPA-600/2-77-064c (NTIS PB-272107) U.S. Environmental Protection Agency., Cincinnati, OH., pp. 107.

MAPAMA, 2017. *Tramos de ríos de España clasificados según Pfafstetter modificado*. https://www.miteco.gob.es/es/cartografia-y-sig/ide/descargas/agua/red-hidrografica.aspx (accessed 24 March 2018).

Martínez-Ibarra, E., 2012. A geographical approach to post-flood analysis: The extreme flood event of 12 October 2007 in Calpe (Spain). Applied Geography. 32, 490-500. https://doi.org/10.1016/j.apgeog.2011.06.003.

Mein, R.G., Larson, C.L., 1973. Modeling infiltration during a steady rain. Water Resources Research. 9, 384-394. https://doi.org/10.1029/WR009i002p00384.

Miao, Q., Yang, D., Yang, H., Li, Z., 2016. Establishing a rainfall threshold for flash flood warnings in China's mountainous areas based on a distributed hydrological model. Journal of Hydrology. 541, 371-386. https://doi.org/10.1016/j.jhydrol.2016.04.054.

Michaud, J., Sorooshian, S., 1994. Comparison of simple versus complex distributed runoff models on a midsized semiarid watershed. Water Resources Research. 30, 593-605. https://doi.org/10.1029/93WR03218.

Michaud, J.D., Hirschboeck, K.K., Winchell, M., 2001. Regional variations in small-basin floods in the United States. Water Resources Research. 37, 1405-1416. https://doi.org/10.1029/2000WR900283.

Molina-Sanchis, I., Lázaro, R., Arnau-Rosalén, E., Calvo-Cases, A., 2016. Rainfall timing and runoff: The influence of the criterion for rain event separation. Journal of Hydrology and Hydromechanics. 64, 226-236. https://doi.org/10.1515/johh-2016-0024.

Morote-Seguido, A.F., Hernández-Hernández, M., 2017. El uso de aguas pluviales en la ciudad de Alicante. De viejas ideas a nuevos enfoques. Papeles de Geografía. 63, 1-19. http://dx.doi.org/10.6018/geografia/2016/267531.

Nearing, M.A., Liu, B.Y., Risse, L.M., Zhang, X., 1996. Curve numbers and Green-Ampt effective hydraulic conductivities. Journal of the American Water Resources

Association (JAWRA). 32, 125-136. http://dx.doi.org/10.1111/j.1752-1688.1996.tb03440.x.

Nguyen, C.C., Gaume, E., Payrastre, O., 2014. Regional flood frequency analyses involving extraordinary flood events at ungauged sites: further developments and validations. Journal of Hydrology. 508, 385-396. http://dx.doi.org/10.1016/j.jhydrol.2013.09.058.

Neitsch, S.L., Arnold, J.G., Kiniry, J.R., Williams, J.R., 2011. Soil and Water Assessment Tool. Theorical Documentation. Version 2009. Texas Water Resources Institute, Texas.

Nogueira de Andrade, M.M., Szlafsztein, C.F., 2018. Vulnerability assessment including tangible and intangible components in the index composition: An Amazon case study of flooding and flash flooding. Science of The Total Environment. 630, 903-912. https://doi.org/10.1016/j.scitotenv.2018.02.271.

Olcina-Cantos, J., Hernández-Hernández, M., Rico-Amorós, A.M., Martínez-Ibarra, E., 2010. Increased risk of flooding on the coast of Alicante (Region of Valencia, Spain). Natural Hazards and Earth System Sciences. 10, 2229-2234. https://doi.org/10.5194/nhess-10-2229-2010.

Overton, D.E., 1966. Muskingum flood routing of upland streamflow. Journal of Hydrology. 4, 185-200. https://doi.org/10.1016/0022-1694(66)90079-5.

Pagán, J.I., López, M., López, I., Tenza-Abril, A.J., Aragonés, L., 2018. Causes of the different behaviour of the shoreline on beaches with similar characteristics. Study case of the San Juan and Guardamar del Segura beaches, Spain. Science of The Total Environment. 634, 739-748. https://doi.org/10.1016/j.scitotenv.2018.04.037.

Papagiannaki, K., Lagouvardos, K., Kotroni, V., Bezes, A., 2015. Flash flood occurrence and relation to the rainfall hazard in a highly urbanized area. Natural Hazards and Earth System Sciences. 15, 1859-1871. https://doi.org/10.5194/nhess-15-1859-2015.

Park, Y., Pachepsky, Y., Hong, E.M., Shelton, D., Coppock, C., 2016. Escherichia coli release from streambed to water column during baseflow periods: A modeling study. Journal of Environmental Quality. 46, 219-226. https://doi.org/10.2134/jeq2016.03.0114.

PATRICOVA., 2015. *Plan de acción territorial sobre prevención del riesgo de inundación en la Comunidad Valenciana* (PATRICOVA). *Dirección General de Ordenación del Territorio, Urbanismo y Paisaje*, Valencia.

Pérez-González, M.L., Capra-Pedol, L., Dávila-Hernández, N., Borselli, L., Solís-Valdez, S., Ortiz-Rodríguez, A.J., 2017. Spatio-temporal land-use changes in the Colima-Villa de Álvarez metropolitan area, and their relationship to floodings. Revista Mexicana de Ciencias Geológicas. 34, 78-90. http://dx.doi.org/10.22201/cgeo.20072902e.2017.2.435.

Pérez-Morales, A., Gil-Guirado, S., Olcina-Cantos, J., 2015. Housing bubbles and the increase of flood exposure. Failures in flood risk management on the Spanish south-eastern coast (1975-2013). Journal of Flood Risk Management. 11, S302-S313. http://dx.doi.org/10.1111/jfr3.12207.

Perrin, C., Michel, C., Andréassian, V., 2001. Does a large number of parameters enhance model performance? Comparative assessment of common catchment model structures on 429 catchments. Journal of Hydrology. 242, 275-301. https://doi.org/10.1016/S0022-1694(00)00393-0.

Pulido-Velazquez, M., Peña-Haro, S., García-Prats, A., Mocholi-Almudever, A.F., Henriquez-Dole, L., Macian-Sorribes, H., Lopez-Nicolas, A., 2015. Integrated assessment of the impact of climate and land use changes on groundwater quantity and quality in the Mancha Oriental system (Spain). Hydrol. Earth Syst. Sci. 19, 1677-1693. https://doi.org/10.5194/hess-19-1677-2015.

R-CRAN, 2018. R: A language and environment for statistical computing. https://cran.r-project.org/ (accessed 2 March 2018).

Rodrigo-Comino, J., Martínez-Hérnandez, C., Iserloh, T., Cerdá, A., 2018. Contrasted impact of land abandonment on soil erosion in Mediterranean agriculture fields. Pedosphere. 28, 617-631. https://doi.org/10.1016/S1002-0160(17)60441-7.

ROEA, 2018. *Red Oficial de Estaciones de Aforo*. https://www.miteco.gob.es/es/cartografia-y-sig/ide/descargas/agua/anuario-de-aforos.aspx (accessed 8 April 2018).

Romero-Díaz, A., Ruiz-Sinoga, J.D., Robledano-Aymerich, F., Brevik, E.C., Cerdà, A., 2017. Ecosystem responses to land abandonment in western Mediterranean mountains. Catena. 149, 824-835. https://doi.org/10.1016/j.catena.2016.08.013.

Rouholahnejad, E., Abbaspour, K.C., Srinivasan, R., Bacu, V., Lehmann, A., 2014. Water resources of the Black Sea Basin at high spatial and temporal resolution. Water Resour. Res. 50, 5866-5885. https://doi.org/10.1002/2013WR014132.

Rozalis, S., Morin, E., Yair, Y., Price, C., 2010. Flash flood prediction using an uncalibrated hydrological model and radar rainfall data in a Mediterranean watershed under changing hydrological conditions. Journal of Hydrology. 394, 245-255. https://doi.org/10.1016/j.jhydrol.2010.03.021.

SAIH, 2018. *Sistema Automático de Información Hidrológica*. https://www.miteco.gob.es/es/agua/temas/evaluacion-de-los-recursos-hidricos/SAIH/ (accessed 8 April 2018).

Sánchez-Galiano, J.C., Martí-Ciriquián, P., Fernández-Aracil, P., 2017. Temporary population estimates of mass tourism destinations: The case of Benidorm. Tourism Management. 62, 234-240. https://doi.org/10.1016/j.tourman.2017.04.012.

Scorpio, V., Crema, S., Marra, F., Righini, M., Ciccarese, G., Borga, M., Cavalli, M., Corsini, A., Marchi, L., Surian, N., Comiti, F., 2018. Basin-scale analysis of the geomorphic effectiveness of flash floods: A study in the northern Apennines (Italy). Science of The Total Environment. 640, 337-351. https://doi.org/10.1016/j.scitotenv.2018.05.252.

SCS., 1986. Urban Hydrology for Small Watersheds. In: Release-55. SCSEDUSDoAT, (Eds.), pp. 164.

Sharpley, A.N., Williams, J.R. 1990. EPIC-Erosion/Productivity Impact Calculator: 1. Model documentation. U.S. Department of Agriculture, Agricultural Research Service.

Sheskin, D.J., 2007. Handbook of parametric and nonparametric statistical procedures.

SIA, 2018. *Sistema de Información del Anuario de Aforos*. https://www.miteco.gob.es/es/agua/temas/evaluacion-de-los-recursos-hidricos/sistema-informacion-anuario-aforos/ (accessed 8 April 2018).

Silvestro, F., Rebora, N., Cummings, G., Ferraris, L. 2017. Experiences of dealing with flash floods using an ensemble hydrological nowcasting chain: implications of communication, accessibility and distribution of the results. Journal of Flood Risk Management. 10, 446-462. https://doi.org/10.1111/jfr3.12161.

Sonnen, M.B. 1980. Urban runoff quality: Information needs. Journal of the Technical Councils, ASCE. 106, 29-40.

Tarboton, D.G., Bras, R.L., Rodriguez-Iturbe, I., 1991. On the extraction of channel networks from digital elevation data. Hydrological Processes. 5, 81-100. https://doi.org/10.1002/hyp.3360050107.

Valdes-Abellan, J., Pardo, M.A., Tenza-Abril, A.J., 2017. Observed precipitation trend changes in the western Mediterranean region. International Journal of Climatology. 37, 1285-1296. https://doi.org/10.1002/joc.4984.

Williams, J.R., 1995. The EPIC Model. In: Singh VP, Ed. Computer Models of Watershed Hydrology. Water Resources Publications, Highlands Ranch, CO., pp. 909-1000.

Winchell, M., Srinivasan, R.S., Di Luzio, M., Arnold, J.G., 2013. ArcSWAT Interface for SWAT2012. User's Guide. Texas Water Resources Institute, Texas.

Yang, X., Liu, Q., He, Y., Luo, X., Zhang, X., 2015. Comparison of daily and sub-daily SWAT models for daily streamflow simulation in the Upper Huai River Basin of China. Stochastic Environmental Research and Risk Assessment. 30, 959-972. https://doi.org/10.1007/s00477-015-1099-0.

Zhong, S., Yang, L., Toloo, S., Wang, Z., Tong, S., Sun, X., Crompton, D., FitzGerald, G., Huang, C., 2018. The long-term physical and psychological health impacts of flooding: A systematic mapping. Science of The Total Environment. 626, 165-194. https://doi.org/10.1016/j.scitotenv.2018.01.041.

Table 1

Main features of ravine basins.

Basin	Surface (km^2)	Maximum altitude (m.a.s.l.)*	Average slope (%)	Soils		Land use	
				Dominant soil/Associated soils and inclusions	% area	Categories	% area
Agua Amarga	64.5	551	11.8	Haplic calcisols/haplic gypsisols	91.5	Urban	9.3
				Haplic gypsisols/calcaric regosols	7.1	Agricultural	46.2
				Haplic calcisols/chromic luvisols	0.8	Natural	44.6
				Calcaric cambisols/chromic luvisols	0.6		
Oveja	200.9	1281	13.6	Calcaric cambisols/chromic luvisols	15.8	Urban	15.0
				Haplic gypsisols/calcaric regosols	12.9	Agricultural	27.3
				Haplic calcisols/haplic gypsisols	10.5	Natural	57.7
				Haplic calcisols/chromic luvisols	10.9		
				Calcaric cambisols/calcaric regosols	24.7		
				Haplic calcisols/lithic leptosols	25.1		
Alicante Puerto	21.1	212	4.0	Calcaric cambisols/chromic luvisols	96.1	Urban	75.5
				Haplic calcisols/haplic gypsisols	3.9	Agricultural	23.8
						Natural	0.7
Juncaret	68.2	566	8.3	Calcaric cambisols/calcaric regosols	27.5	Urban	30.9
				Lithic leptosols/ calcaric cambisols	11.7	Agricultural	30.0
				Calcaric cambisols/chromic luvisols	60.7	Natural	39.1
San Juan	10.2	113	2.2	Calcaric cambisols/chromic luvisols	91.2	Urban	76.1
				Calcaric cambisols/calcaric regosols	8.8	Agricultural	23.5
						Natural	0.5

*m.a.s.l: meters above sea level.

Table 2

Corine Land Cover land use classes reclassified into SWAT land use classes (Baseline, 1990, 2000, 2006 and 2012 scenarios) and overland Manning's roughness coefficients according to the Engman (1986) categories.

CLC Code	Land use class	SWAT Code	Land use class	Overland Manning's Roughness (n_{ov})	
				Value	Category
111	Continuous urban fabric	URHD	Residential-High Density	0.03	No tillage
112	Discontinuous urban fabric	URML	Residential-Med/low Density	0.04	No tillage
121	Industrial or commercial units	UCOM	Commercial	0.04	No tillage
122	Road and rail networks and associated land	UTRN	Transportation	0.04	No tillage
123	Port areas	UCOM	Commercial	0.04	No tillage
124	Airports	UTRN	Transportation	0.04	No tillage
131	Mineral extraction sites	UIDU	Industrial	0.03	No tillage
132	Dump sites	UIDU	Industrial	0.03	No tillage
133	Construction sites	URLD	Residential-low Density	0.05	No tillage
141	Green urban areas	URLD	Residential-low Density	0.05	No tillage
142	Sport and leisure facilities	UCOM	Commercial	0.04	No tillage
211	Non-irrigated arable land	AGRL	Agricultural land-generic	0.16	Short grass prairie
212	Permanently irrigated land	AGRC	Agricultural land-close-grown	0.19	Conventional tillage
221	Vineyards	GRAP	Vineyard	0.21	Conventional tillage
222	Fruit trees and berry plantations	ORCD	Orchard	0.60	Rangeland
223	Olive groves	OLIV	Olives	0.22	Conventional tillage
231	Pastures	PAST	Pasture	0.60	Rangeland
242	Complex cultivation patterns	AGRR	Agricultural Land-Row Crops	0.22	Conventional tillage
243	Land principally occupied by agriculture, with significant areas of natural vegetation	AGRL	Agricultural land-generic	0.16	Short grass prairie
312	Coniferous forest	FRSE	Forest-Evergreen	0.60	Rangeland
321	Natural grassland	RNGE	Range-Grasses	0.24	Dense grass
323	Sclerophyllous vegetation	SWRN	Southwestern Arid Range	0.11	Chisel plow
324	Transitional woodland-shrub	RNGB	Range-Brush	0.60	Rangeland
333	Sparsely vegetated areas	BARR	Barren	0.12	Chisel plow
523	Sea and ocean	WATR	Water	0.01	-

Table 3

Weighted average curve number II dependent on main land use categories of the Baseline, 1990, 2000, 2006 and 2012 scenarios.

Basin	Land use										Curve number II				
	Categories	Scenario Baseline		Scenario 1990		Scenario 2000		Scenario 2006		Scenario 2012		Scenario Baseline	Scenario 1990	Scenario 2000	Scenario 2006	Scenario 2012
		Surface (km^2)	% area	Surface (km^2)	% area	Surface (km^2)	% area	Surface (km^2)	% area	Surface (km^2)	% area					
Agua Amarga	Urban	0.0	0.0	0.6	0.9	3.2	4.9	4.1	6.3	6.0	9.3	-	83.4	84.9	84.0	86.8
	Agricultural	47.8	74.1	47.2	73.2	44.5	69.0	43.7	67.7	29.8	46.2	54.0	54.0	52.4	52.3	56.3
	Natural	16.7	25.9	16.7	25.9	16.8	26.1	16.8	26.0	28.8	44.6	46.9	46.9	47.3	47.4	49.8
Oveja	Urban	0.0	0.0	11.2	5.6	23.2	11.5	23.9	11.9	30.1	15.0	-	83.5	85.3	87.0	88.1
	Agricultural	121.1	60.3	113.1	56.3	99.3	49.5	98.7	49.1	54.8	27.3	59.4	59.7	57.7	57.7	58.9
	Natural	79.8	39.7	76.6	38.1	78.4	39.0	78.3	39.0	116.0	57.7	49.2	49.3	50.0	50.1	51.8
Alicante Puerto	Urban	0.0	0.0	9.0	4.2.9	11.6	55.1	13.2	62.5	15.9	75.5	-	84.6	84.9	87.6	88.6
	Agricultural	19.1	90.3	10.4	49.3	8.7	41.1	7.1	33.8	5.0	23.8	59.1	58.6	58.0	57.5	53.0
	Natural	2.0	9.7	1.6	7.8	0.8	3.8	0.8	3.8	0.1	0.7	45.0	45.5	42.7	42.9	51.6
Juncaret	Urban	0.0	0.0	8.6	12.6	13.5	19.8	15.3	22.4	21.0	30.9	-	81.3	83.0	85.2	89.2
	Agricultura	53.	78	45.		41.		39.		20.		64.1	64.0	64.1	64.3	58.6

	l	4	.3	3	6	3	6	7	5	5	3	57.2	58.1	58.8	58.8	60.2
	Natural	14.8	21.7	14.3	6.4	13.4	0.5	13.2	8.2	26.7	0.0					
					21.0		19.7		19.4		39.1					
	Urban		0.0		27.9		60.6		67.9		76.1					
	Agricultural	0.0		2.8		6.2		6.9		7.8		-	86.6	84.5	86.2	86.5
San Juan		10.2	100.0	7.4	72.1	4.0	39.4	3.3	32.1	2.3	23.5	61.0	61.2	60.3	59.7	60.2
	Natural	0.0		0.0		0.0		0.0		0.1		-	-	-	-	51.1
			0.0		0.0		0.0		0.0		0.5					

Table 4

Kruskal-Wallis ANOVA analysis of the storm hydrographs achieved at subbasin outlets in the coastline.

Basin	DF*	Chi-squared	P-value
Agua Amarga	4	6.8729	0.1428
Oveja	4	5.3666	0.2517
Alicante Puerto	4	83.354	<0.0001
Juncaret	4	24.507	<0.0001
San Juan	4	48.409	<0.0001

*DF: degrees of freedom.

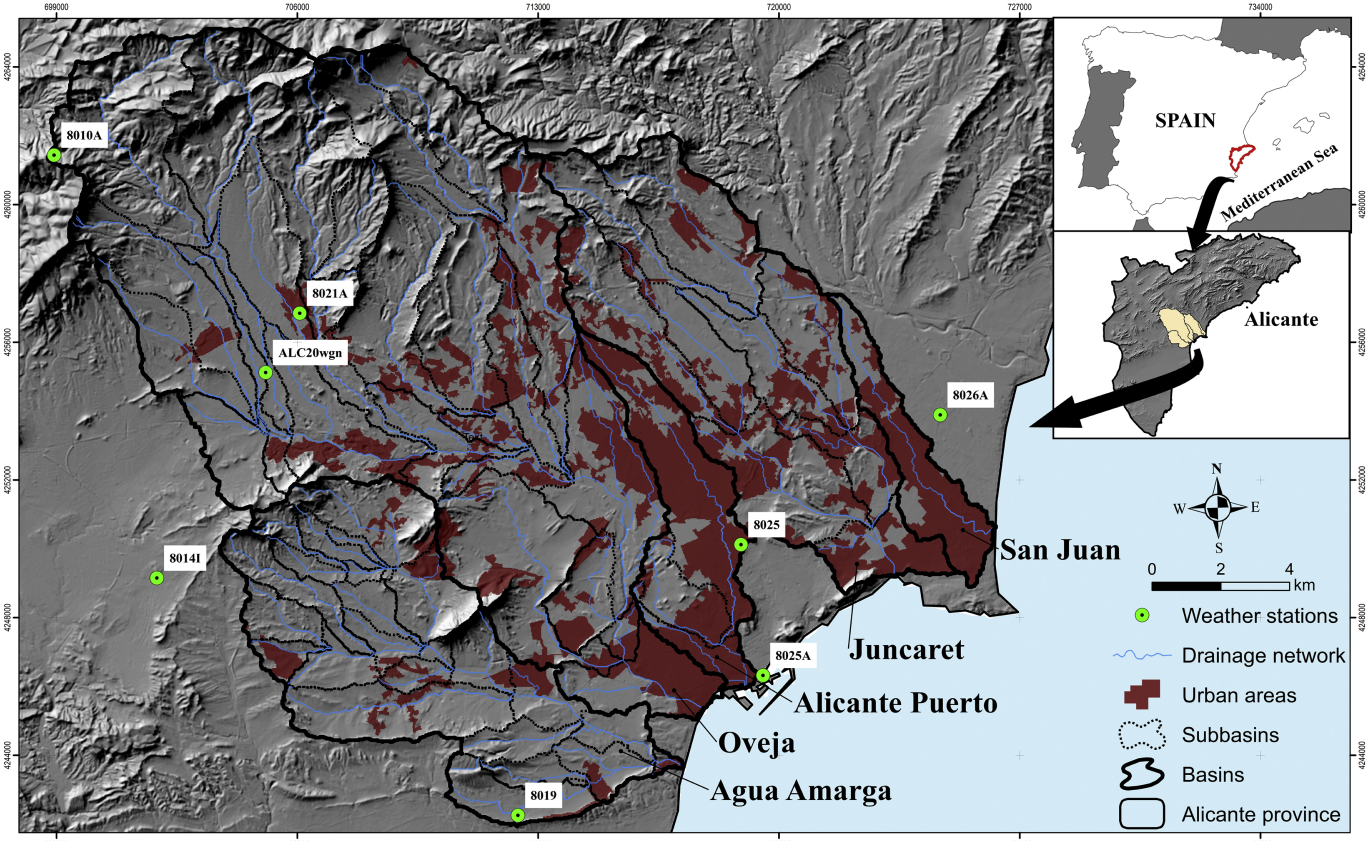
699000
706000
713000
720000
727000
734000
4256000
4252000
4248000
4244000
8010A
8021A
ALC20wgn
8026A
8025
8014I
San Juan
8025A
Juncaret
Alicante Puerto
Oveja
Agua Amarga
8019
SPAIN
Mediterranean Sea
Alicante
N
W
E
S
0
2
4
km
Weather stations
Drainage network
Urban areas
Subbasins
Basins
Alicante province

Figure 1

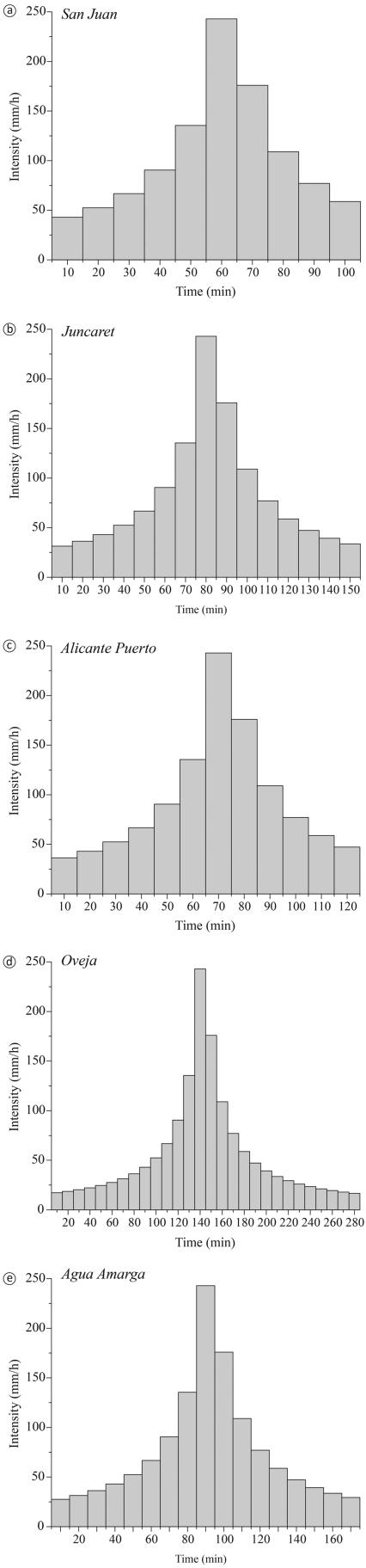
a
San Juan
Intensity (mm/h)
Time (min)
b
Juncaret
Intensity (mm/h)
Time (min)
c
Alicante Puerto
Intensity (mm/h)
Time (min)
d
Oveja
Intensity (mm/h)
Time (min)
e
Agua Amarga
Intensity (mm/h)
Time (min)

Figure 2

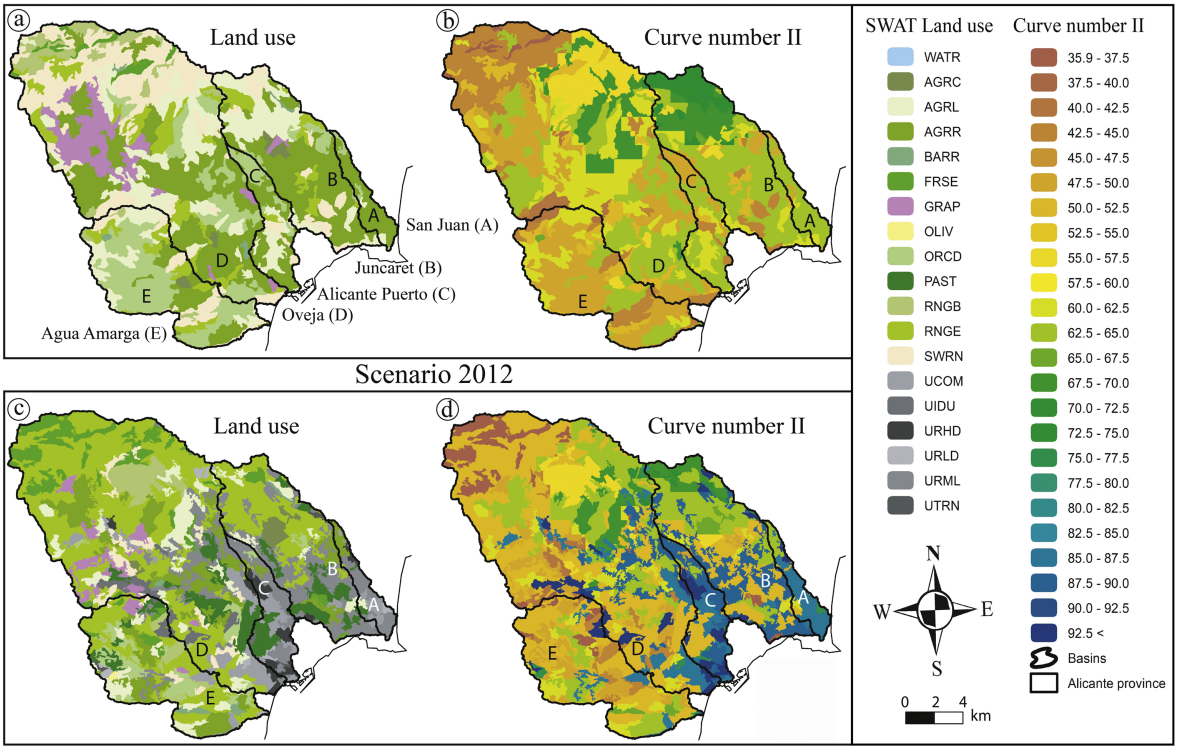
Scenario baseline
a
Land use
b
Curve number II
San Juan (A)
Juncaret (B)
Alicante Puerto (C)
Oveja (D)
Agua Amarga (E)
Scenario 2012
c
Land use
d
Curve number II
SWAT Land use
WATR
AGRC
AGRL
AGRR
BARR
FRSE
GRAP
OLIV
ORCD
PAST
RNGB
RNGE
SWRN
UCOM
UIDU
URHD
URLD
URML
UTRN
Curve number II
35.9 - 37.5
37.5 - 40.0
40.0 - 42.5
42.5 - 45.0
45.0 - 47.5
47.5 - 50.0
50.0 - 52.5
52.5 - 55.0
55.0 - 57.5
57.5 - 60.0
60.0 - 62.5
62.5 - 65.0
65.0 - 67.5
67.5 - 70.0
70.0 - 72.5
72.5 - 75.0
75.0 - 77.5
77.5 - 80.0
80.0 - 82.5
82.5 - 85.0
85.0 - 87.5
87.5 - 90.0
90.0 - 92.5
92.5 <
Basins
Alicante province
N
W
E
S
0 2 4
km

Figure 3

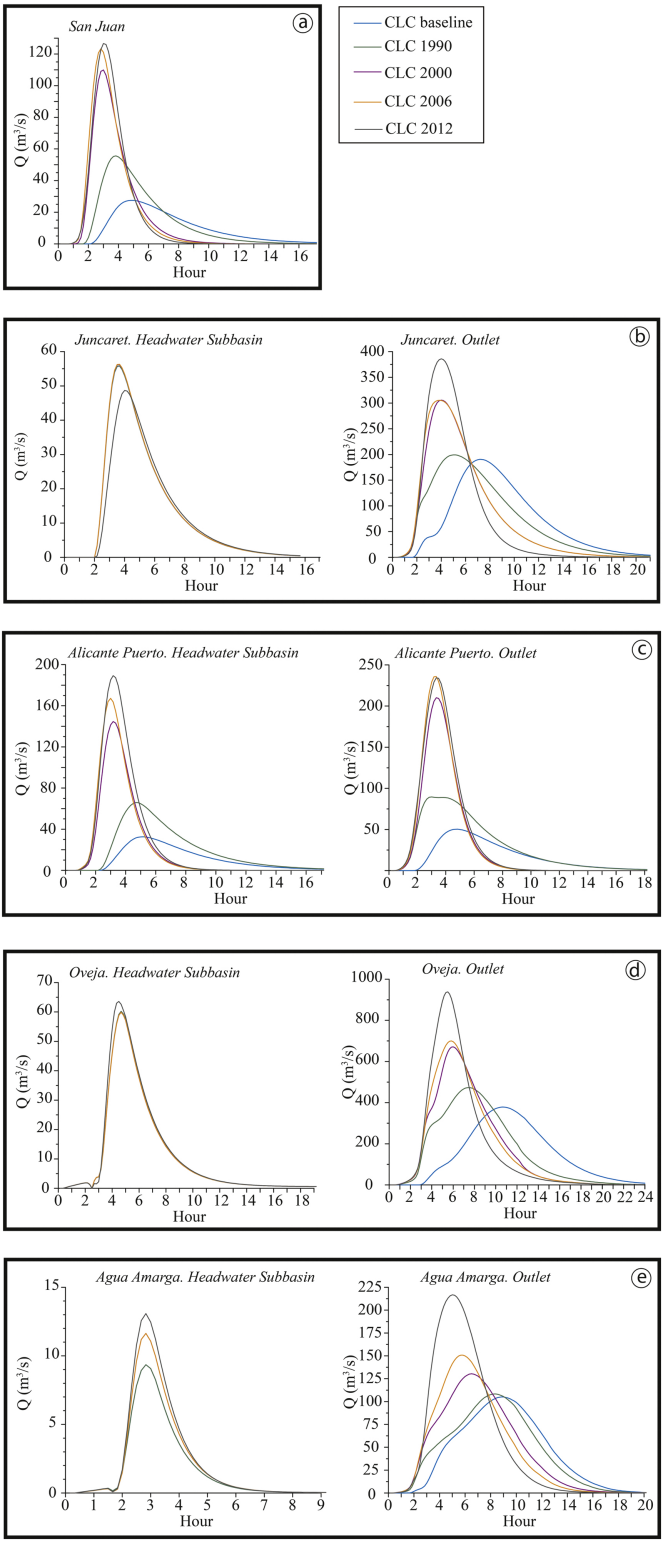
San Juan
a
CLC baseline
CLC 1990
CLC 2000
CLC 2006
CLC 2012
Q (m³/s)
Hour
Juncaret. Headwater Subbasin
Juncaret. Outlet
b
Alicante Puerto. Headwater Subbasin
Alicante Puerto. Outlet
c
Oveja. Headwater Subbasin
Oveja. Outlet
d
Agua Amarga. Headwater Subbasin
Agua Amarga. Outlet
e

Figure 4

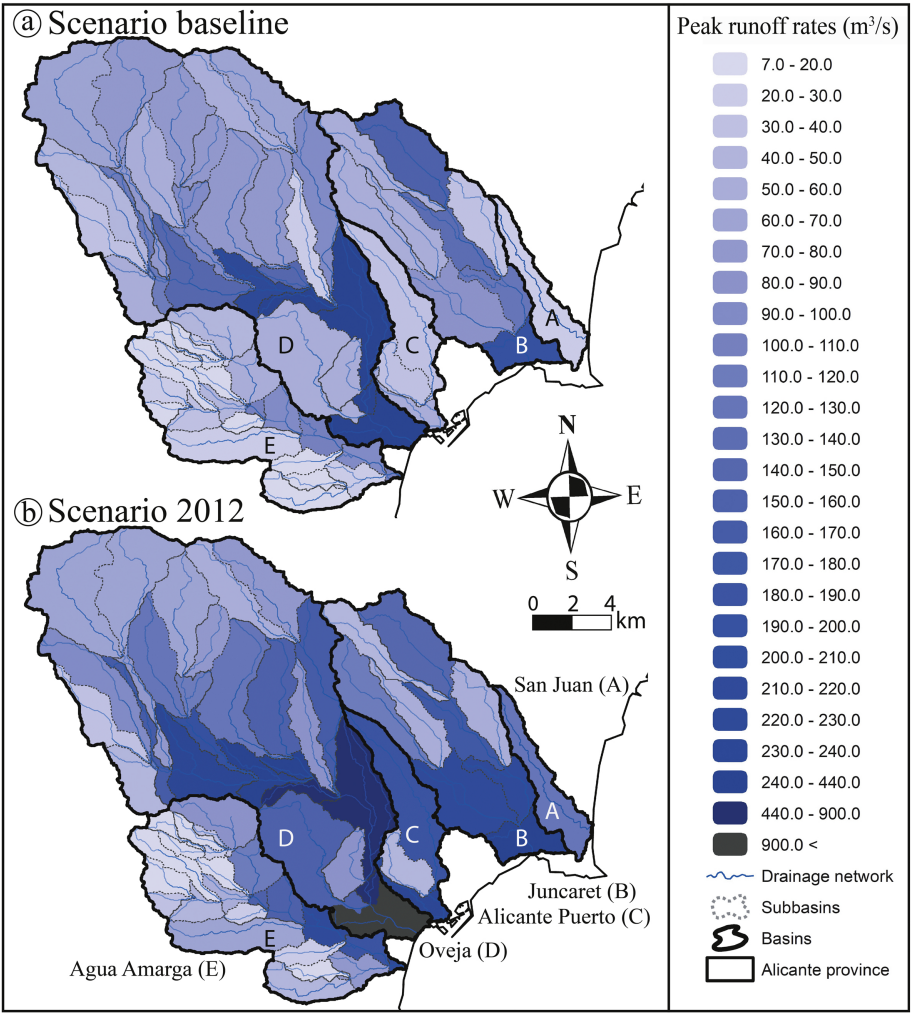
ⓐ Scenario baseline
ⓑ Scenario 2012
A
B
C
D
E
N
W
E
S
0 2 4
km
San Juan (A)
Juncaret (B)
Alicante Puerto (C)
Oveja (D)
Agua Amarga (E)
Peak runoff rates (m³/s)
7.0 - 20.0
20.0 - 30.0
30.0 - 40.0
40.0 - 50.0
50.0 - 60.0
60.0 - 70.0
70.0 - 80.0
80.0 - 90.0
90.0 - 100.0
100.0 - 110.0
110.0 - 120.0
120.0 - 130.0
130.0 - 140.0
140.0 - 150.0
150.0 - 160.0
160.0 - 170.0
170.0 - 180.0
180.0 - 190.0
190.0 - 200.0
200.0 - 210.0
210.0 - 220.0
220.0 - 230.0
230.0 - 240.0
240.0 - 440.0
440.0 - 900.0
900.0 <
Drainage network
Subbasins
Basins
Alicante province

Figure 5

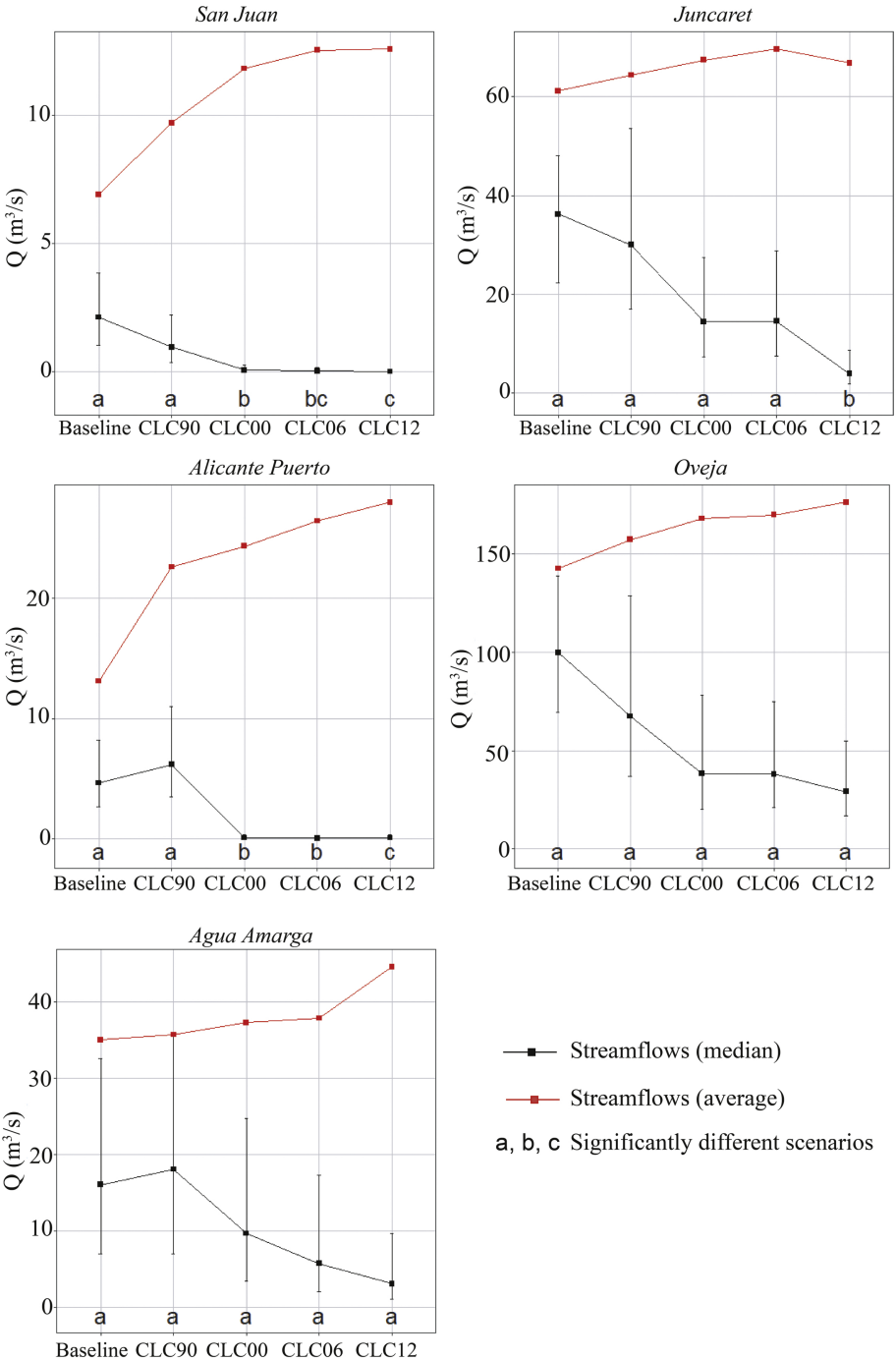
San Juan
Q (m³/s)
10
5
0
a a b bc c
Baseline CLC90 CLC00 CLC06 CLC12
Juncaret
Q (m³/s)
60
40
20
0
a a a a b
Baseline CLC90 CLC00 CLC06 CLC12
Alicante Puerto
Q (m³/s)
20
10
0
a a b b c
Baseline CLC90 CLC00 CLC06 CLC12
Oveja
Q (m³/s)
150
100
50
0
a a a a a
Baseline CLC90 CLC00 CLC06 CLC12
Agua Amarga
Q (m³/s)
40
30
20
10
0
a a a a a
Baseline CLC90 CLC00 CLC06 CLC12
Streamflows (median)
Streamflows (average)
a, b, c Significantly different scenarios

Figure 6